

Generative Adversarial Networks in Ultrasound Imaging: Extending Field of View Beyond Conventional Limits

Matej Gazda^{1,4}, Samuel Kadoury^{3,4,5}, Jakub Gazda², and Peter Drotar¹

¹IISLab, Technical University of Kosice, Slovakia

²2nd Department of Internal Medicine, Pavol Jozef Šafárik University and Louis Pasteur University Hospital, Košice, Slovakia

³Universite de Montreal, Montreal, Canada

⁴MedICAL Laboratory, Polytechnique Montreal, Montreal, Canada

⁵Centre de recherche du CHUM (CRCHUM), Montreal, Canada

ABSTRACT

Transthoracic Echocardiography (TTE) is a fundamental, non-invasive diagnostic tool in cardiovascular medicine, enabling detailed visualization of cardiac structures crucial for diagnosing various heart conditions. Despite its widespread use, TTE ultrasound imaging faces inherent limitations, notably the trade-off between field of view (FoV) and resolution. This paper introduces a novel application of conditional Generative Adversarial Networks (cGANs), specifically designed to extend the FoV in TTE ultrasound imaging while maintaining high resolution. Our proposed cGAN architecture, termed echoGAN, demonstrates the capability to generate realistic anatomical structures through outpainting, effectively broadening the viewable area in medical imaging. This advancement has the potential to enhance both automatic and manual ultrasound navigation, offering a more comprehensive view that could significantly reduce the learning curve associated with ultrasound imaging and aid in more accurate diagnoses. The results confirm that echoGAN reliably reproduce detailed cardiac features, thereby promising a significant step forward in the field of non-invasive cardiac navigation and diagnostics.

Introduction

Transthoracic Echocardiography (TTE) Ultrasound (USG) is a cornerstone diagnostic tool in cardiovascular medicine, valued for its non-invasive approach and ability to comprehensively assess cardiac anatomy and function. It enables detailed visualization of cardiac structures, such as chambers, valves, and myocardium, and is essential in diagnosing conditions like heart failure, valvular heart disease, and cardiomyopathies. One of TTE USG's key advantages is its capacity for real-time dynamic imaging, allowing clinicians to observe cardiac motion and provide insights beyond what static imaging can offer.

Despite its wide applications, TTE USG has inherent limitations, particularly in the trade-off between field of view (FoV) and resolution. Achieving high resolution in a focused area typically results in a narrower FoV, providing detailed imagery at the cost of a broader view. Conversely, a wider FoV can reduce the resolution, compromising detail for a more comprehensive perspective. This balance between FoV and resolution is a crucial consideration in clinical ultrasound imaging.

Different ultrasound probes are tailored for specific medical purposes. Linear array probes are effective for shallow structures, while curvilinear array probes are suited for deeper tissue imaging. Endocavitary probes excel in specialized fields such as urology and gynecology, offering high-resolution images of internal structures. Sector array probes, often used in cardiac imaging, balance FoV with depth. However, these probes still confront the challenge of balancing FoV, resolution, and penetration depth.

In this context, our research has explored the application of a conditional Generative Adversarial Networks (cGANs) to extend the FoV in TTE USG imaging while maintaining high resolution. The proposed cGAN architecture, denoted as echoGAN, is capable of generating realistic anatomical structures through outpainting, thereby broadening the viewable area in medical imaging. This approach aims to address the limitations in FoV and resolution trade-offs, potentially enhancing both automatic and manual ultrasound navigation. For automatic navigation¹, an expanded FoV can provide a more comprehensive view, potentially improving the efficiency and accuracy of imaging processes, especially in complex diagnostic scenarios.

Furthermore, this extended FoV could be particularly beneficial for less experienced physicians in manual navigation. The study by Chisholm et al.² and the work of Vinodh et al.³ focus on cardiac ultrasound training, specifically evaluating the duration of training necessary to achieve proficiency in TTE. These studies demonstrate that mastering TTE requires a considerable amount of time. By offering a wider yet detailed view, our cGAN-based approach could reduce the learning curve

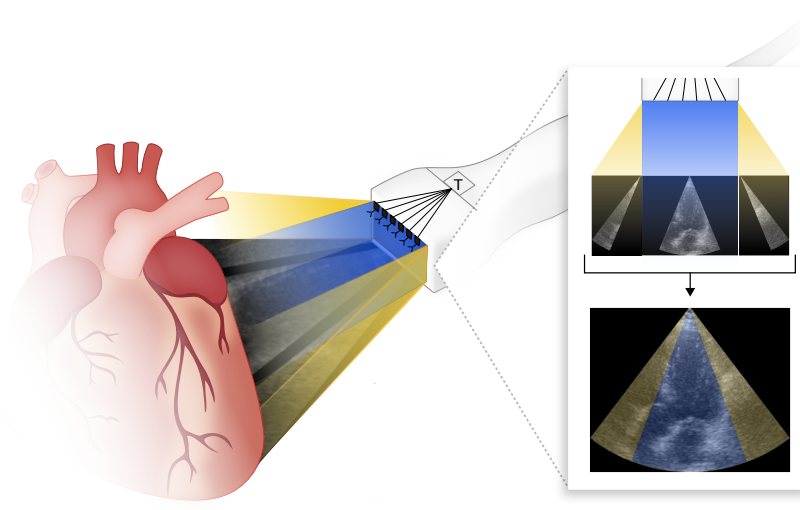


Figure 1. Extending field of view (yellow) vs basic (teal)

associated with ultrasound imaging and assist in making more accurate diagnoses. This is especially relevant in cases requiring both detailed examination and broader assessments.

Guidance during ultrasound imaging, especially in echocardiography, presents significant challenges. While previous studies, such as the one by Li et al.⁴, have explored automated robotic navigation in Transesophageal Echocardiography (TEE) with limited degrees of freedom, similar challenges persist in TTE. The complex nature of cardiac anatomy and the need for precise imaging in both TEE and TTE demand high expertise and skill from echocardiographers³.

In conventional TEE examinations, the echocardiographer manually guides the probe to acquire standard views of the heart's anatomy, as outlined in guidelines by Hahn et al.⁵. This process involves intricate navigation, as the echocardiographer must rely on their interpretation of ultrasound images and a mental model of the heart's spatial layout. Achieving proficiency in this task requires substantial training and experience. Similarly, in TTE, despite the non-invasive nature of the procedure, obtaining optimal imaging planes is a complex skill. The echocardiographer must maneuver the probe on the patient's chest, often working within limited space and requiring a nuanced understanding of cardiac structures and their orientation. This complexity is heightened by the variability in patients' anatomy and the need to adjust probe positions to capture clear images of specific cardiac areas.

Both TEE and TTE share the common challenge of probe navigation, heavily reliant on the operator's skill and understanding of cardiac anatomy. The difficulty lies in aligning the ultrasound beam with the heart's structures to obtain the necessary views for accurate diagnosis. This process is often not straightforward and demands a high level of dexterity and spatial awareness. Given these challenges, there is a continuous search for technological advancements that can aid in simplifying the navigation process, making echocardiography more accessible and reliable, especially for less experienced practitioners.

Overall, proposed advancement in TTE USG technology through the integration of cGANs significantly contribute to the field of non-invasive cardiac diagnostics. By addressing some of the fundamental limitations of current ultrasound technology, this approach holds the promise of improving navigation processes and in turn patient care in cardiology. The showcase of the novel approach proposed in this paper is depicted in Fig. 1.

In ultrasound imaging, clinicians have the capability to manipulate the field of view to enhance image resolution. This is achieved through the focusing of the ultrasound beam, which can be narrowed to increase the lateral resolution at specific depths, known as the focal zone. By adjusting the focus and consequently decreasing the FoV, the ultrasound system can provide a more detailed view of the area of interest. This technique is particularly useful in cardiac imaging, where high resolution is critical for accurate diagnosis. The adjustment of the FoV and focus is an integral part of ultrasound knobology,

allowing for optimization of image quality based on the clinical requirements of the examination⁶.

In the domain of medical imaging, particularly ultrasound imaging, the task of outpainting introduces a set of unique challenges that are markedly distinct from those encountered in the outpainting of general or natural images⁷⁻⁹. The paramount requirement for anatomical accuracy in medical images necessitates that outpainting algorithms not only generate visually plausible extensions but also ensure these extensions accurately represent the expected anatomy. This is crucial, as any deviation could compromise the clinical utility of the image. Moreover, ultrasound images are characterized by specific textures and patterns that denote various tissues, fluids, and pathological conditions. Ensuring continuity in these textures and patterns during the outpainting process is essential, yet challenging, as the algorithm must replicate medical characteristics that might be absent from the portion of the image initially visible. This is further complicated by the imperative to maintain diagnostic integrity; the outpainted areas must not introduce artifacts or inaccuracies that could lead to misinterpretation or misdiagnosis.

Results

Dataset

The data utilised in this study comprises clinical examinations derived from 500 patients, obtained at the University Hospital of St Etienne in France collected under the CAMUS project¹⁰. The data acquisitions were aimed to facilitate Left Ventricular Ejection Fraction (LVEF) measurements. For each patient, 2D apical fourchamber and two-chamber view sequences were recorded. The images were extracted from video recordings yielding in average 20 images per patient (min 10, max 42). Altogether 9964 images constitute the final dataset. From these, 7917 corresponding to 400 patients were used for training of generative adversarial network. To avoid data leakage, it was ensured that data from the same patient are present only in training or only in testing dataset, not both.

Outpainting the Ultrasound FoV

The present study proposed GAN for extending the FoV in echocardiography to enhance both manual and automatic navigation. From computer vision perspective is FoV extension formulated as outpainting problem. Outpainting seeks for a semantically consistent extension of the input image beyond its available content. The outpainting process involves the GAN generating new pixels and features in a way that seamlessly integrates with the existing content, maintaining the anatomical and contextual coherence of the cardiac structures.

This approach not only promises to refine navigation accuracy but also to facilitate a more comprehensive understanding of the heart's structure and function. Enhancing the FoV through outpainting addresses a critical gap in cardiac imaging by ensuring that the right heart is not overlooked, thus supporting more informed clinical decision-making. Our findings could mark a significant step forward in non-invasive cardiac diagnostics, offering a novel solution to the longstanding challenge of incomplete cardiac visualization during echocardiography.

In Fig. 2, we provide visual samples of outpainted images generated by the echoGAN. These examples showcase the network's ability to extrapolate relevant cardiac features beyond the visible boundaries, demonstrating the ability of the proposed GAN architecture to enhance the overall imaging capabilities in echocardiography. The visual representations serve to illustrate the effectiveness of the echoGAN in creating realistic and contextually coherent extensions of the original ultrasound images, thereby contributing to the advancement of FoV extension techniques in cardiac imaging applications.

To quantitatively measure the quality of outpainted images we utilised Fréchet Inception Distance (FID). The average FID for outpainted images, when using 30 degree wide cut for inference was equal to 122.08.

Different size of extended view

We evaluated the influence of the training cone size on the quality of outpainted sections in ultrasound images. Figure 3 illustrate two distinct scenarios: the first utilizes a narrower 10-degree cone cut as the inference input, with the echoGAN algorithm tasked with generating outpainted extensions that span 40 degrees on both sides; the second employs a 60-degree cone cut for inference, with outpainting applied to 15-degree segments on each side. Notably, the generated images appear highly realistic, even when echoGAN is interfaced with only a 10-degree cut. The algorithm demonstrates ability to reproduce cardiac muscle structures with high fidelity. This is particularly evident in the first, second, and fourth rows, where echoGAN successfully outpaints a complete right atrium, that is an encouraging result given that the right atrium was not included in the 10-degree cut, suggesting that echoGAN can reconstruct it entirely. In the case of the left ventricle and left atrium, we observe that echoGAN is capable of outpainting the missing boundary parts for the 30-degree cut and can significantly reconstruct substantial portions of these structures for the 10-degree cut. Again, to quantitatively evaluate the quality of outpainted USG images, we measure FID for different sizes of outpainted regions. The results are provided in Tab. 1. The 30 degree cut means, that echoGAN generates 15 degrees on both sides. Similarly in case of 80 degrees, echoGAN generates 40 degree on both sides, using only very narrow 10 degree cone as an input.

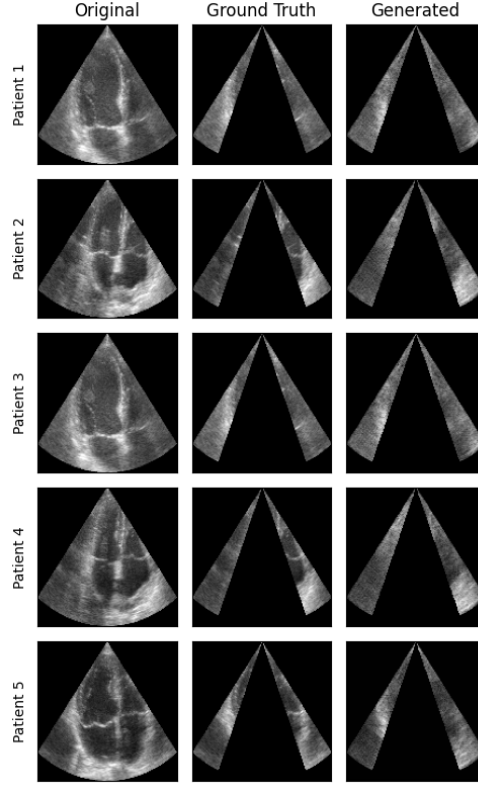


Figure 2. Several examples from different patients on ground truth image and outpainted image.

	Cut 30	Cut 46	Cut 60	Cut 80
FID	122.08	143.83	145.74	149.63

Table 1. The average FID for different sizes of outpainted area.

As expected, the smaller FID values indicating better similarity are achieved for the cases when the broader cut is used as an input for network inference.

Right ventricle area

The majority of diagnostic, prognostic, and monitoring efforts in cardiology traditionally emphasize the analysis of the left heart due to its direct role in systemic circulation. However, comprehensive echocardiographic assessment necessitates detailed examination of the entire heart, including the right ventricle (RV), which plays a pivotal role in pulmonary circulation and systemic venous return¹¹. During standard echocardiography, capturing the complete anatomy of the right heart can be challenging. The RV, in particular, may be partially or entirely outside the ultrasound beam’s FoV, limiting the accuracy and completeness of the examination. Despite the primary focus on the left heart in clinical practice, quantification of right heart parameters is crucial in various clinical scenarios.

Our experiments are specifically aimed at the quantification of the RV area from both original and outpainted echocardiograms. The rationale for focusing on the RV area is influenced by the established practice in cardiology where, for instance, the measurement of left ventricular ejection fraction incorporates the left ventricular area as a crucial parameter in its evaluation¹². Drawing inspiration from such methodologies, we hypothesize that if the RV areas derived from generated (outpainted) and real echocardiograms are similar, it would substantiate the utility and validity of the generated images for clinical and diagnostic purposes.

Moreover, accurate assessment of RV size and function is paramount in conditions such as Pulmonary Hypertension, various Cardiomyopathies, and Right Ventricular Infarction, where the right heart’s performance directly influences patient outcomes¹¹.

In our experimental setup, both the original and the artificially generated echocardiograms were manually annotated to obtain segmentation masks. This process allowed for precise comparison of RV volumes, assessing the efficacy and accuracy

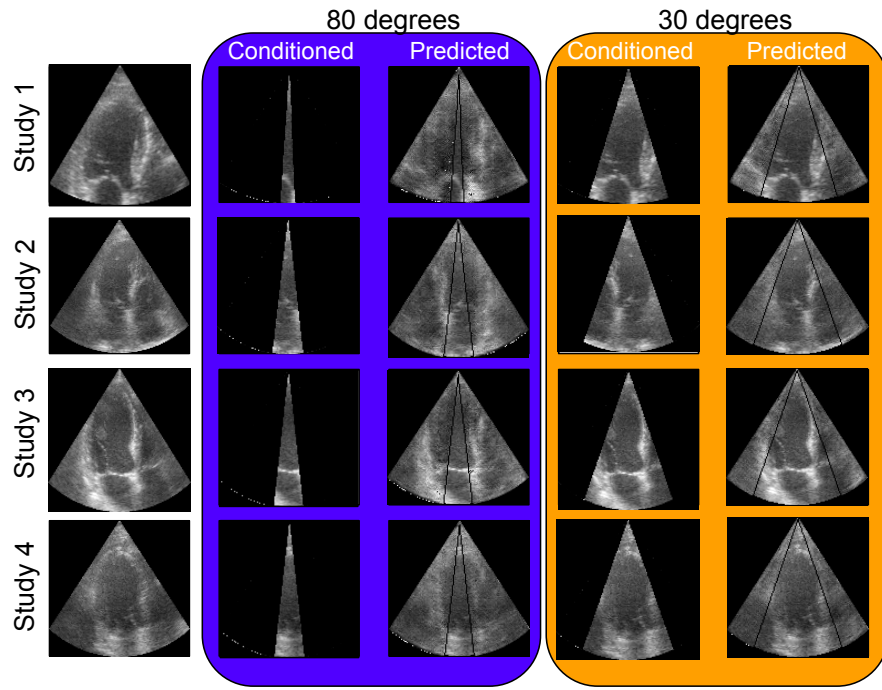


Figure 3. Extending field of view (yellow) vs basic (teal) for 30 and 80 degree outpainting.

of GAN-based outpainting in reproducing anatomically coherent extensions of the cardiac structures. By comparison of the RV volumes derived from the conventional and outpainted echocardiograms, this experiment aims to validate the potential of echoGANs in overcoming the intrinsic limitations of current echocardiography practices. Comparison of segmentation for RV on original and on outpainted image is in Fig. 4 and Fig. 5.

We performed the Wilcoxon signed-rank test to compare the RV areas obtained from the original and the outpainted echocardiograms. The results of this test confirmed the null hypothesis, indicating that there is no statistically significant difference between the RV areas measured in the original echocardiographic images and those derived from images extended through echoGAN outpainting. This finding validates the accuracy and effectiveness of the GAN-based outpainting technique in echocardiography. The ability of GANs to generate anatomically coherent extensions of the cardiac structures without compromising the integrity of the images suggests that this approach can reliably extend the field of view in echocardiographic navigation.

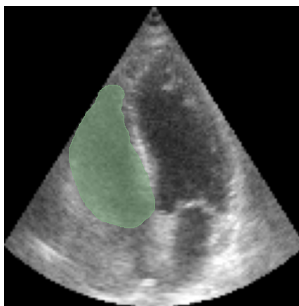


Figure 4. Segmentation over Right Ventricle for GT 4CH view with

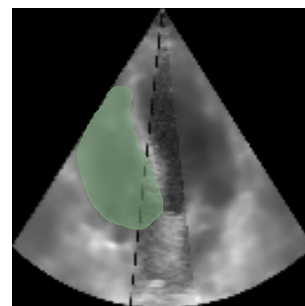


Figure 5. Segmentation of outpainted RV with 80 degrees cut for the same 4CH view

Discussion

One of the main limitations of our study is limited data. The dataset used, while extensive, may not fully capture the diversity of cardiac pathologies or patient demographics typically encountered in broader clinical practice. This limitation could affect the generalizability of our findings, as the performance of the echoGAN might vary with different or more heterogeneous datasets. Moreover, while the echoGAN architecture demonstrates the ability to generate anatomically plausible images, there remains a risk of generating artifacts, especially in more complex or ambiguous cardiac regions. These potential inaccuracies necessitate further refinement of the model and algorithms to ensure reliability and clinical utility.

Additionally, a prevalent limitation of publicly available datasets is their focus on specific traditional views like apical two-chamber (A2C) and apical four-chamber (A4C), while neglecting other standard views such as parasternal (parasternal long axis (PLAX), parasternal short axis (PSAX)) and subcostal views (subcostal 4CH and subcostal short axis). Moreover, these datasets completely omit images captured from non-standard views, which are often not even recorded as they are primarily used for navigation purposes.

To address this limitation, future work could incorporate shape priors derived from medical imaging modalities that capture comprehensive chest information, such as CT or MRI. Alternatively, the dataset could be expanded with images from non-standard views generated through real-time ultrasound simulation solutions from CTs or MRIs, as demonstrated in¹³. In addition to physics-based simulators, unpaired image-to-image translation methods like mUNIT¹⁴ or CycleGAN¹⁵ could be employed. While paired image-to-image translation might yield superior results, the required data is rarely available.

Directly outpainting ultrasound views using scanline data could be a faster and more precise approach, provided that access to the probe hardware and controls were available, which is currently not feasible. However, oversampling the area near the probe and heavily extrapolating at the end of the scanning volume could introduce errors. Should this capability become available, it would offer a promising avenue for further exploration.

Methods

Image preprocessing

Due to the absence of US data in raw format within the dataset, our analysis is confined to the final, scan-converted images. Similar approach might be implemented in raw data as well. In our endeavor to facilitate outpainting, we meticulously segmented the cone from the image data through the application of conventional image processing techniques. Initially, we located the first non-zero pixel from the top as a means to identify the tip of the probe. Subsequently, we delineated the furthest left and right boundaries emanating from the probe to the edge of the image. By determining the angular relationship between these boundaries, we systematically removed segments measuring 15, 23, 30, and 40 degrees from each side in a symmetrical fashion. The resulting masks, corresponding to the excised segments, were preserved for further analysis.

As for the preprocessing during the training, we just scaled the intensity into [0, 1] interval.

echoGAN architecture

The proposed GAN architecture consists of two neural networks : generator and discriminator.

- a) As a generator we employed U-Net architecture, as introduced by Ronneberger et al.¹⁶. It features two input channels: one for the masked image and the other for the binary mask, which indicates the regions for outpainting. It is configured with four downsampling layers, each characterized by specific kernel sizes [7, 5, 5, 5] and strides [1, 2, 2, 2], optimizing the network's capacity for feature extraction and image reconstruction within the designated areas.
- b) The Discriminator employs a conventional Convolutional Neural Network (CNN) design, structured with a sequence of channels [1, 32, 64, 128, 128] and uniform strides [1, 2, 2, 2] across layers, with a kernel size consistently set to 3. This configuration enables effective differentiation between generated and authentic images, ensuring the generative model's outputs closely mimic the target distribution.

This network, depicted on Fig. 6, is trained by combination of two different loss functions: adversarial loss function and learned perceptual image patch similarity. The adversarial loss consists of two components: one for the discriminator (\mathcal{L}_D) and one for the generator (\mathcal{L}_G). The discriminator loss \mathcal{L}_D is designed to correctly distinguish between real and fake images, while the generator loss \mathcal{L}_G aims to fool the discriminator into classifying fake images as real. The adversarial loss for the discriminator can be formulated as:

$$\mathcal{L}_D = -\mathbb{E}_{x \sim p_{\text{data}}(x)}[\log D(x)] - \mathbb{E}_{x \sim p_{\text{data}}(x), m}[\log(1 - D(G(x \odot (1 - m), m)))] \quad (1)$$

where x represents the real images sampled from the data distribution, m is the mask, and $x \odot (1 - m)$ denotes the image with the masked area removed. Generator loss is then denoted as

$$\mathcal{L}_G = -\mathbb{E}_{x \sim p_{\text{data}}(x), m}[\log D(G(x \odot (1 - m), m))]. \quad (2)$$

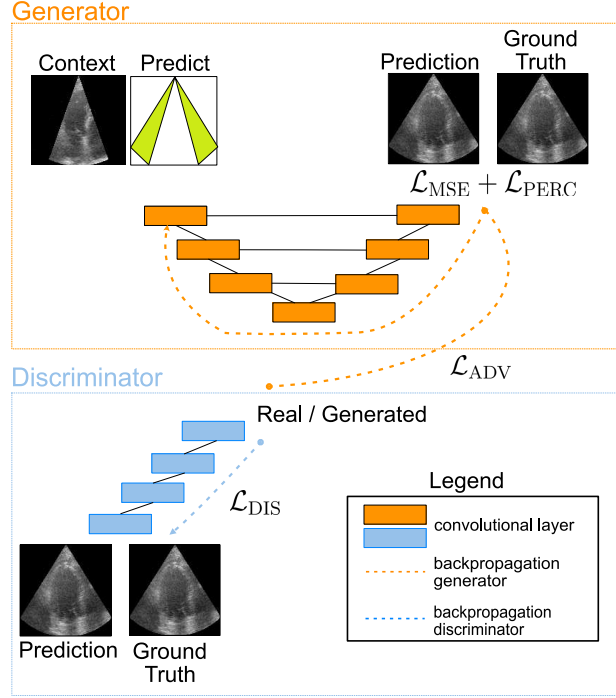


Figure 6. Proposed echoGAN Architecture

The Learned Perceptual Image Patch Similarity (LPIPS) metric evaluates the perceptual similarity between two images in a way that is more aligned with human visual perception than traditional metrics like MSE. The general form of the LPIPS equation involves computing differences in deep feature representations extracted from the two images being compared, then weighting and summing these differences to produce a final similarity score. LPIPS is defined as

$$\mathcal{L}_{\text{LPIPS}} = \sum_l w_l \cdot \frac{1}{H_l W_l C_l} \sum_{h,w,c} \|\phi_l(I^1)_{h,w,c} - \phi_l(I^2)_{h,w,c}\|_2^2 \quad (3)$$

where l is the layer of the deep feature extractor, H accounts for height, W for width, C for number of channels, ϕ is the featured extractor (pretrained VGG16).

Final loss for generation is then a summation of both losses

$$\mathcal{L} = \mathcal{L}_G + \mathcal{L}_{\text{LPIPS}}. \quad (4)$$

Experimental design

To quantitatively assess the quality of generated images Fréchet Inception Distance¹⁷ was employed. FID aims to capture the perceptual similarity between real and generated images by considering their feature representations extracted from a pre-trained Inception CNN. FID calculates the Fréchet distance between multivariate Gaussian distributions fitted to the feature representations of real and generated images. Formally is FID defined as

$$\text{FID} = \|\mu_{\text{real}} - \mu_{\text{gen}}\|^2 + \text{Tr}(\sum_{\text{real}} + \sum_{\text{gen}} - 2(\sum_{\text{real}} \sum_{\text{gen}})^{1/2}), \quad (5)$$

where μ is mean and \sum is covariance of of the feature vectors for the real and generated images respectively. Tr is the trace. A lower FID indicates better similarity between the distributions, suggesting higher image quality and fidelity.

Statistical analysis

To statistically evaluate the difference between the real and AI-generated right ventricle area measurements, we first assessed whether each group of measurements conformed to a normal distribution. This preliminary step involved applying the Shapiro-Wilk test¹⁸, a widely accepted method for testing normality. The results of the Shapiro-Wilk test indicated that the data do not follow a normal distribution, thereby necessitating the selection of a non-parametric statistical test for further analysis.

Consequently, we opted for the Wilcoxon signed-rank test, a non-parametric counterpart to the paired t-test, which is designed for comparing two related samples. This test was employed to examine our hypothesis that there is no significant statistical difference between the areas determined from the AI-generated and real echocardiography data. The choice of the Wilcoxon signed-rank test was appropriate given the non-normal distribution of our data, allowing us to conduct a robust comparison of the median values between the two groups without the assumption of normality. The statistical analysis was conducted using the Python programming language, utilizing the SciPy library.

References

1. Soemantoro, R., Kardos, A. & Tang, G. An ai-powered navigation framework to achieve an automated acquisition of cardiac ultrasound images. *Sci Rep* **13** (2023).
2. Chisholm, C. B. *et al.* Focused cardiac ultrasound training: how much is enough? *The J. emergency medicine* **44**, 818–822 (2013).
3. Nanjaya, V. B. *et al.* Levels of training in critical care echocardiography in adults. recommendations from the college of intensive care medicine ultrasound special interest group. *Australas. J. Ultrasound Medicine* **22**, 73–79 (2019).
4. Li, K., Li, A., Xu, Y., Xiong, H. & Meng, M. Q.-H. RI-tee: Autonomous probe guidance for transesophageal echocardiography based on attention-augmented deep reinforcement learning. *IEEE Transactions on Autom. Sci. Eng.* (2023).
5. Hahn, R. T. *et al.* Guidelines for performing a comprehensive transesophageal echocardiographic examination: recommendations from the american society of echocardiography and the society of cardiovascular anesthesiologists. *J. Am. Soc. Echocardiogr.* **26**, 921–964 (2013).
6. Ng, A. & Swanevelder, J. Resolution in ultrasound imaging. *Continuing Educ. Anaesthesia, Critical Care & Pain* **11**, 186–192 (2011).
7. Cheng, Y.-C. *et al.* Inout: Diverse image outpainting via gan inversion. In *2022 IEEE/CVF Conference on Computer Vision and Pattern Recognition (CVPR)*, 11421–11430, DOI: [10.1109/CVPR52688.2022.01114](https://doi.org/10.1109/CVPR52688.2022.01114) (2022).
8. Li, J., Chen, C. & Xiong, Z. Contextual outpainting with object-level contrastive learning. In *Proceedings of the IEEE/CVF Conference on Computer Vision and Pattern Recognition (CVPR)*, 11451–11460 (2022).
9. Wang, Y., Wei, Y., Qian, X., Zhu, L. & Yang, Y. Rego: Reference-guided outpainting for scenery image. *IEEE Transactions on Image Process.* **33**, 1375–1388, DOI: [10.1109/TIP.2024.3357290](https://doi.org/10.1109/TIP.2024.3357290) (2024).
10. Leclerc, S. *et al.* Deep learning for segmentation using an open large-scale dataset in 2d echocardiography. *IEEE Transactions on Med. Imaging* **38**, 2198–2210, DOI: [10.1109/TMI.2019.2900516](https://doi.org/10.1109/TMI.2019.2900516) (2019).
11. Zaidi, A. *et al.* Echocardiographic assessment of the right heart in adults: a practical guideline from the british society of echocardiography. *Echo Res Pract* **7** (2020).
12. Motazedian, P., Marbach, J., Prosperi-Porta, G., Parlow, S. & Santo, P. D. Diagnostic accuracy of point-of-care ultrasound with artificial intelligence-assisted assessment of left ventricular ejection fraction. *npj Digit. Med.* **6** (2023).
13. Shams, R., Hartley, R. & Navab, N. Real-time simulation of medical ultrasound from ct images. In *Medical Image Computing and Computer-Assisted Intervention–MICCAI 2008: 11th International Conference, New York, NY, USA, September 6–10, 2008, Proceedings, Part II 11*, 734–741 (Springer, 2008).
14. Huang, X., Liu, M.-Y., Belongie, S. & Kautz, J. Multimodal unsupervised image-to-image translation. In *Proceedings of the European conference on computer vision (ECCV)*, 172–189 (2018).
15. Zhu, J.-Y., Park, T., Isola, P. & Efros, A. A. Unpaired image-to-image translation using cycle-consistent adversarial networks. In *Proceedings of the IEEE international conference on computer vision*, 2223–2232 (2017).
16. Ronneberger, O., Fischer, P. & Brox, T. U-net: Convolutional networks for biomedical image segmentation. In *Medical Image Computing and Computer-Assisted Intervention–MICCAI 2015: 18th International Conference, Munich, Germany, October 5–9, 2015, Proceedings, Part III 18*, 234–241 (Springer, 2015).
17. Dowson, D. & Landau, B. The fréchet distance between multivariate normal distributions. *J. multivariate analysis* **12**, 450–455 (1982).
18. Razali, N. M. & Wah, Y. B. Power comparisons of Shapiro-Wilk, Kolmogorov-Smirnov, Lilliefors and Anderson-Darling tests. *J. Stat. Model. Anal.* **2** (2011).

Acknowledgements (not compulsory)

Author contributions statement

Must include all authors, identified by initials, for example: A.A. conceived the experiment(s), A.A. and B.A. conducted the experiment(s), C.A. and D.A. analysed the results. All authors reviewed the manuscript.

Additional information

To include, in this order: **Accession codes** (where applicable); **Competing interests** (mandatory statement).

The corresponding author is responsible for submitting a [competing interests statement](#) on behalf of all authors of the paper. This statement must be included in the submitted article file.